KSME

Springer

Journal of Mechanical Science and Technology 35 (12) 2021

Original Article
DOI 10.1007/s12206-021-1143-6

Keywords:
· Fuel injection rate
· Fuel injection duration
· Fuel rail pressure (FRP)
· Gasoline direct injection (GDI)
· High pressure fuel pump (HPFP)
· Signal to noise (SN) ratio

Correspondence to:
Choong Hoon Lee
chlee5@seoultech.ac.kr

Citation:
Lee, B. J., Lee, C. H. (2021). Fuel injection rate and its variation of a GDI injector operated in engine motoring conditions. Journal of Mechanical Science and Technology 35 (12) (2021) 5741~5751.
http://doi.org/10.1007/s12206-021-1143-6

Received March 7th, 2021
Revised September 5th, 2021
Accepted September 6th, 2021

† Recommended by Editor
Tong Seop Kim

Fuel injection rate and its variation of a GDI injector operated in engine motoring conditions

Byoung Jin Lee and Choong Hoon Lee

Department of Mechanical and Automotive Engineering, Seoul National University of Science and Technology, Seoul 01811, Korea

Abstract The cylinder head assembly from a GDI engine was separated to build a GDI fuel injection system capable of controlling the rail pressure and fuel injection levels. The GDI fuel injection system is driven by a three-phase AC motor with a direct connection between the camshaft and the motor. The operating conditions of the GDI fuel injection system are equivalent to those of actual engine driving. The AC motor drives the GDI high-pressure fuel pump by rotating the engine camshaft. In the GDI high-pressure fuel pump (HPFP), fuel is pressurized on the upward stroke of the plunger and pumped to the fuel rail. Fuel rail pressure (FRP) control is possible by controlling the opening/closing timing of the HPFP's pressure control valve (PCV), the fuel injection duration and the camshaft speed. In order to calculate the fuel injection rate characteristics of the GDI injector statistically under fixed conditions of the camshaft speed, FRP, and injection duration, the measurements of the fuel injection rate were repeated at regular time intervals. To calculate the variation of the fuel injection rate, the S/N (signal-to-noise) ratio, which is the average FRP divided by the FRP standard deviation, was calculated. A fuel injection rate was obtained under 88 experimental conditions combining the three conditions of the HPFP's PCV opening/closing timing, fuel injection duration, and camshaft rotational speed. The smaller S/N ratio shows the larger FRP variation. Also, it was identified that the S/N ratio is related to the variation of the fuel injection rate.

1. Introduction

The basic configurations of the fuel injection systems used in recent gasoline engines and diesel engines are nearly identical. In other words, both gasoline engines and diesel engines tend to use fuel injection systems based on a common rail and electronically controlled injectors. Only the common rail pressure is different. Gasoline engines using the port fuel injection (PFI) system maintain a constant rail pressure of almost 0.4 MPa. On the other hand, the rail pressure of the GDI engine is controlled in the range of 3 MPa to 35 MPa depending on the engine operating conditions [1-4]. The rail pressure of a diesel engine is controlled in the range of 20 MPa to 200 MPa depending on the engine operation [5].

Compared to the gasoline PFI method and the diesel common rail method, the fuel pressurization method of the GDI engine has a problem in that the fuel rail pressure fluctuates. In the PFI method, the fuel pump uses a gear type or a roller type to pressurize the fuel stably. The high-pressure pump of a diesel engine usually is driven by means of three plungers, and when the eccentric cam rotates once, it delivers high-pressure fuel three times. On the other hand, the GDI HPFP uses a single plunger pump and delivers high-pressure fuel to the common rail 3-4 times for every rotation of the driving camshaft. For this reason, the FRP pulsation by the GDI single plunger pump is relatively large. The FRP by the GDI single-plunger pump increases the fuel injection rate variation and causes problems related to the durability and stability of the GDI fuel supply system as well as noise and vibration. At higher engine speeds, these problems are amplified. Despite the various problems caused by pressure pulsation stemming

from the GDI single-plunger high-pressure pump, it continues to be the most commonly used type in GDI engines due to its simple structure and small size [6-10].

Fuel rail pressure control is an important task during the evaluation of the GDI fuel injection system. Research related to rail pressure control of the GDI fuel injection system mainly relies on the simulation method [11-13]. A study of the FRP and fuel injection characteristics under the operating condition of a GDI engine in Dynamo was also conducted [14-16]. In order to evaluate the GDI fuel injection system, a device that controls the rail pressure identically to how this is done under actual engine operating conditions is required. An integrated control scheme of an experimental rig for a GDI fuel injection system was studied using a FPGA DAQ driven by a PC and a real-time OS [17]. Lee and Lee [18] developed an experimental rig that rotates the camshaft driving a GDI HPFP by directly connecting it to the motor. Lee and Lee [18] studied the effects of the three factors of the camshaft speed, PCV opening/closing timing, and fuel injection duration and how they affect the FRP characteristics using a GDI experimental rig.

It should be noted that the fuel injection rate characteristics have the greatest influence on the fuel economy and emissions of a GDI engine. In the case of a GDI engine, given that fuel is injected directly into the cylinder, the fuel injection rate due to the FRP pulsation greatly influences the combustion characteristics due to the concentration distribution and spatial distribution of the air and fuel mixture. An experimental study related to the fuel injection rate characteristics of a GDI fuel injection system focused on the injectors under the condition of stable rail pressure pulsation [11].

There are two standardized methods for measuring the injection rate of an injector. One measures the static injection rate and the other measures the dynamic injection rate. The static injection rate measures the amount of fuel injected over a period of time with the valve continuously open. In the static injection rate measurement, the injector continuously inject fuel with exciting the injector solenoid for 30 seconds or more. The static injection rate of the injector is one of the important considerations in designing an engine, and it is a standard in calculating the required flow rate under the maximum power output required by the engine [19]. The dynamic injection rate, on the other hand, measures the amount of fuel injected under the condition that the valve opens and closes repeatedly. That is, the same injection is repeated thousands of times and the collected fuel mass is divided by the number of injections to obtain the single injection rate. Usually, when measuring the dynamic injection rate, the injector solenoid excitation time is changed and the frequency of the injection is usually 100 Hz. By measuring the dynamic injection rate while changing the excitation time of the injector solenoid, the linearity of the relationship between the injector excitation time and the injector dynamic injection rate is evaluated (Linear flow range test: LFR test) [19, 20]. In the above-described standardized injector test methods, the injection rate at a constant fuel rail is measured with supplying an electronically controlled driving signal to the injector.

The only difference between PFI and GDI injection rate measurement methods which are standardized is the fuel rail pressure. The rail pressure of the standardized injector tester rig is constant. In the case of a PFI injector, fuel injection is performed under the condition that the fuel rail pressure is maintained constant even under actual engine operating conditions. However, in the real operating GDI engine, the fuel rail pressure is not constant and there are 4 peaks during one camshaft revolution. Factors that affect rail pressure under actual GDI engine operating conditions are engine speed, fuel injection rate, and rail pressure control valve opening/closing timing. The GDI injector injection rate measured with the standardized method [20] is different from the fuel injection rate under the actual GDI engine operating condition. Previous researches on the GDI fuel injection system under the GDI engine operating conditions were mainly achieved by operating the GDI engine on the engine dynamometer. To the authors' knowledge, there has been no research on a measuring device that can measure the fuel injection rate of the GDI injector under the real engine operating conditions. In order to measure the injection rate while controlling the three factors affecting the GDI rail pressure control, the rotation position of the camshaft driving the GDI high-pressure pump must be accurately encoded.

In this study, by modifying the GDI experimental rig of Lee and Lee [18], a system that can accumulate and measure the amount of fuel injected from each injector was developed. The fuel injection rate and FRP pulsation were measured under various experimental conditions controlled by the camshaft speed of the GDI experimental rig, the HPFP PCV opening/closing timing, and the fuel injection duration. Variations of the injection rate according to engine operating conditions were evaluated with the S/N ratio. With the developed measuring device, it is possible to find an optimal fuel injection condition in actual engine operation.

2. Experiments

Fig. 1 shows the schematics of the experimental system used to evaluate the fuel injection rate characteristics and FRP pulsation of the GDI injector. A device capable of measuring the fuel injection rate was added to the experimental system of Lee and Lee [18]. After separating the entire cylinder head assembly, which includes the HPFP, camshaft, and intake and exhaust valves from the GDI engine, the camshaft and three-phase AC motor, the cam shaft was directly connected to the AC motor by means of shaft coupling. When the AC motor rotates one revolution, the camshaft also rotates one revolution. At the other end of the camshaft, the square cam and HPFP are in contact. When the camshaft rotates once, the HPFP's single plunger moves up to four times due to the cam profile and pumps high-pressure fuel to the fuel rail. A rotary encoder is assembled at one end of the AC motor, as shown in Fig. 1. With the A-line of the rotary encoder, 360 square waves are generated for each rotation of the camshaft. Therefore, the

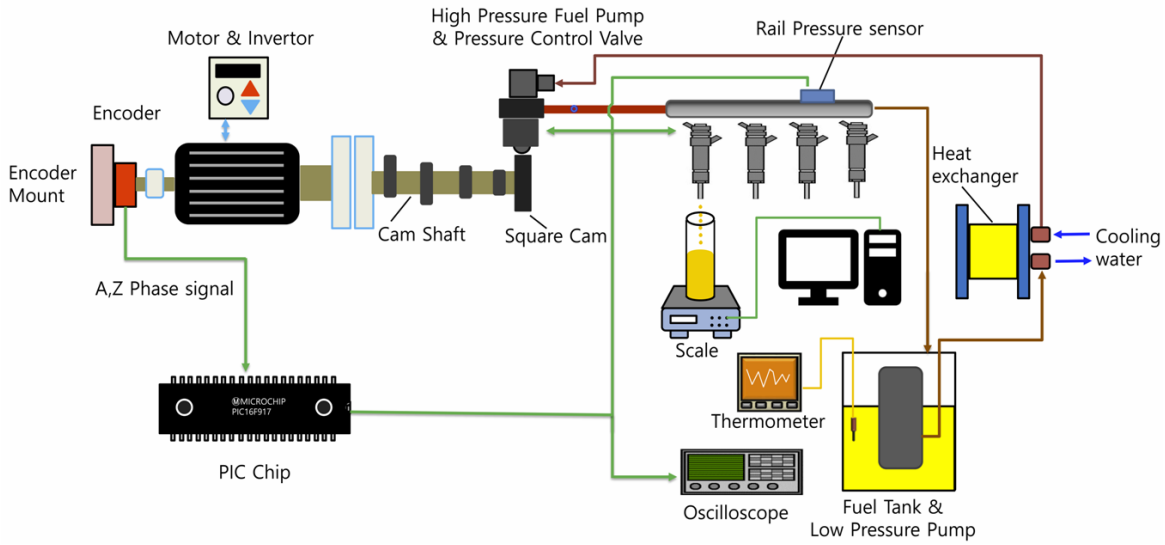

Fig. 1. Experimental setup for evaluating the fuel injection rate and FRP pulsation.

resolution of the encoder is one degree in terms of the cam angle. From the Z-line, one square wave is generated per camshaft rotation and is used as a TDC reference. The encoder's A-line and z-line signals can be input into the microcontroller to measure the camshaft rotation position from the TDC reference. The HPFP's PCV opening/closing timing, fuel injection timing, and fuel injection duration were determined based on the rotary encoder signals.

The fuel supply system consists of a low-pressure fuel pump, the HPFP, the fuel rail, and the injector. The low-pressure fuel pump is immersed in the fuel tank, and its delivery pressure is 0.4 MPa. The fuel from the low-pressure fuel pump is supplied to the fuel rail via the HPFP. The FRP is determined by the combination of the HPFP PCV opening/closing timing, the camshaft speed, and the fuel injection duration. The temperature of the fuel supplied to the fuel pump was maintained at 30 ±2 °C by controlling the amount of cooling water supplied to the heat exchanger. The fuel temperature in the fuel tank was measured using a thermocouple.

The fuel injected from the injector was collected with a mass cylinder and the weight was measured with a scale. For the weight measurement, an OHAUS balance (SPX622KR) with a resolution of 0.01 g was used. The SPX622KR balance transfers the weight of the mass cylinder including the collected fuel to a personal computer at one-second intervals by means of a RS-232C communication link.

The experiment was conducted while changing the camshaft speed at regular intervals under a condition in which the fuel injection duration and HPFP PCV opening/closing timing were both constant. The HPFP PCV opening/closing timing, fuel injection duration, and fuel injection timing were programmed into the microprocessor based on the cam angle. By managing the settings in this way, even if the camshaft speed changes, the HPFP PCV opening/closing timing, fuel injection duration, and fuel injection timing always have constant values based on

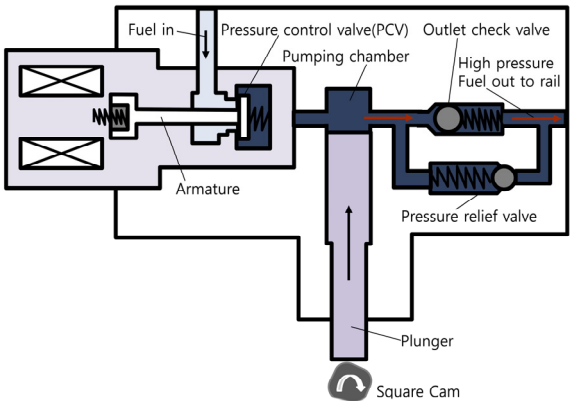

Fig. 2. A schematic diagram of the GDI HPFP used in this study.

the cam angle. After adjusting the target camshaft speed by adjusting the AC motor inverter knob, the rail pressure, A-line, and Z-line signals of the encoder were recorded with a digital oscilloscope, and the fuel injection quantity was also measured at one-second intervals for a certain time. The same experiment was repeated while increasing the camshaft speed by 200 rpm.

Again, the HPFP PCV opening/closing timing and fuel injection duration were programmed into the microprocessor with different values, and the same experiment was repeated. In this study, the injection quantity was measured using one scale, and one injector injected four times for each camshaft rotation. With regard to FRP control, this condition is nearly identical to that used with the four injectors to inject fuel sequentially once per camshaft rotation.

The fuel injection conditions are always the same during the thousands of fuel injections. The developed experimental system is to evaluate the fuel injection rate variation due to the pulsation of the GDI high pressure fuel pump in a fixed engine operating condition.

Fig. 2 shows a schematic diagram of the GDI HPFP used in this study. The schematic diagram of the GDI HPFP by Spegar et al. [11] was modified. Fuel pumping by a single plunger is achieved by rotating the square cam at the end of the camshaft. During the solenoid deactivating duration, the fuel is sucked into the pumping chamber. When the solenoid is activated and the pressure control valve (PCV) moves to the left hand side, this seals the pumping chamber. At the same time, the single plunger moves up to pressurize the fuel in the pumping chamber and the pressurized fuel is supplied to the fuel rail via the outlet check valve. As the solenoid is deactivated, the PCV moves to the right and fuel delivery stops.

The HPFP PCV valve opening angle cases used in the experiment are ATDC 10°, BTDC 89°, BTDC 78°, BTDC 70°, and BTDC 74°, and the closing angle cases are BTDC 70°, BTDC 62°, BTDC 64°, and BTDC 68°. Here, ° refers to the cam angle. The experimental conditions were determined by combining the aforementioned PCV closing and opening angles. The camshaft speed was controlled by increasing it from 400 rpm to 1000 rpm at 200 rpm intervals. Camshaft rotational speeds of 400-1000 rpm correspond to engine rotational speeds of 800-2000 rpm. Given that the engine speed is held to within 2000 rpm under actual vehicle driving conditions, the camshaft rotational speed range of 400-1000 rpm used in this study is suitable. The fuel injection durations used are 4° and 6° in terms of the camshaft angle, and the results after converting the cam angle into time considering the engine speed are summarized in Table 1. Nozzle hole diameter of the GDI injector used in this study is 0.15 mm and number of the nozzle hole is six.

Table 1. Conversion of the fuel injection duration with the cam angle at a certain cam shaft rotation speed into ms.

Cam angle	400 (rpm)	600 (rpm)	800 (rpm)	1000 (rpm)
4°	1.67 (ms)	1.11 (ms)	0.83 (ms)	0.67 (ms)
6°	2.50 (ms)	1.67 (ms)	1.25 (ms)	1.00 (ms)

3. Results and discussion

Fig. 3 shows the average values of the HPFP PCV driving voltage, injector driving voltage, and FRP during one rotation of the camshaft. The measurements are repeated 30 times. The measurements were made under the conditions of a camshaft speed of 400 rpm, HPFP PCV opening and closing angles of 64° and 70°, respectively, a fuel injection duration of 4°, and a fuel injection timing value of BTDC 14°. A Kistler piezo-resistive pressure sensor (4618A2) was used for the FRP measurements. The FRP changes as the camshaft rotation angle position changes. The average FRP during one rotation of the camshaft is approximately 13.3 MPa. The FRP shows four peaks which appear shortly before the single plunger reaches the TDC.

Figs. 4(a)-(e) show the FRP when the HPFP PCV closing timing is fixed and the fuel injection duration and camshaft speed change, respectively. For one fixed HPFP PCV angle, the FRP was measured while changing the opening angle to BTDC 70°, BTDC 74°, BTDC 78°, BTDC 89°, and ATDC 10°. The fixed HPFP PCV closing angle was increased from BTDC 62° to BTDC 70° in 2° increments. In Fig. 4, legends 4 and 6 refer to injection durations of 4° and 6°, respectively. For example, legend 4-O70 means the injection duration is 4° and the PCV opening angle BTDC is 70°. Except for legend O10 (which means ATDC 10°), display legends have the same meanings. Two cases of 4° and 6° for each fuel injection duration were tested. When the HPFP PCV is closed, the rail pressure starts to rise, and when it opens, it drops.

The FRP shown in Figs. 4(a)-(e) became greater as the HPFP PCV closing time was earlier. The HPFP PCV closing was earliest in Fig. 4(a) (PCV closing angle: BTDC 62°) and latest in Fig. 4(e) (PCV closing angle: BTDC 70°). In the camshaft rotational speed range of 400-700 rpm, the FRP change with the HPFP PCV opening angle was clearly observed for a fixed HPFP PCV closing angle. In particular, the FRP showed greater changes as the HPFP PCV closing time was earlier. In the range of 700-1000 rpm, the FRP change with the HPFP

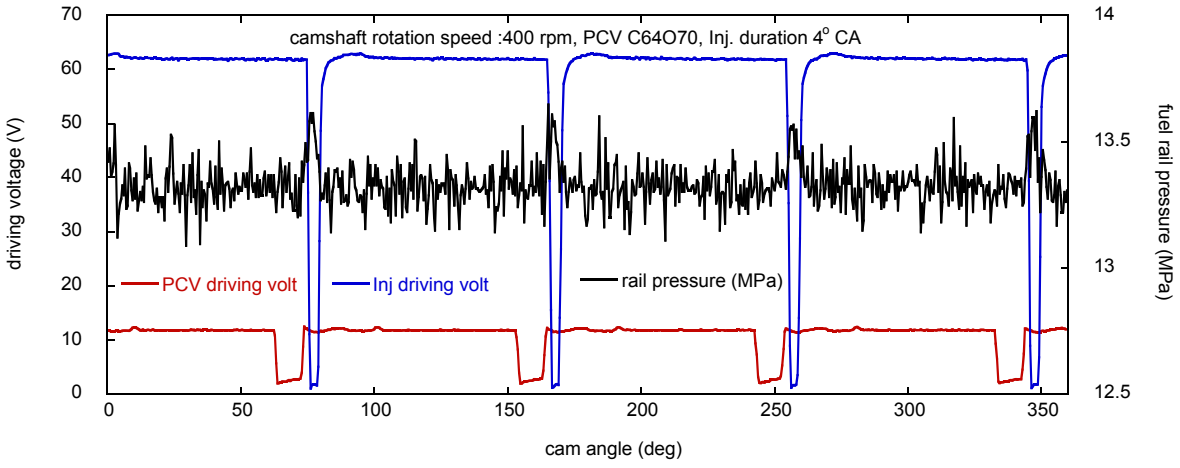

Fig. 3. Average values of the HPFP PCV driving voltage, injector driving voltage and FRP with the cam angle.

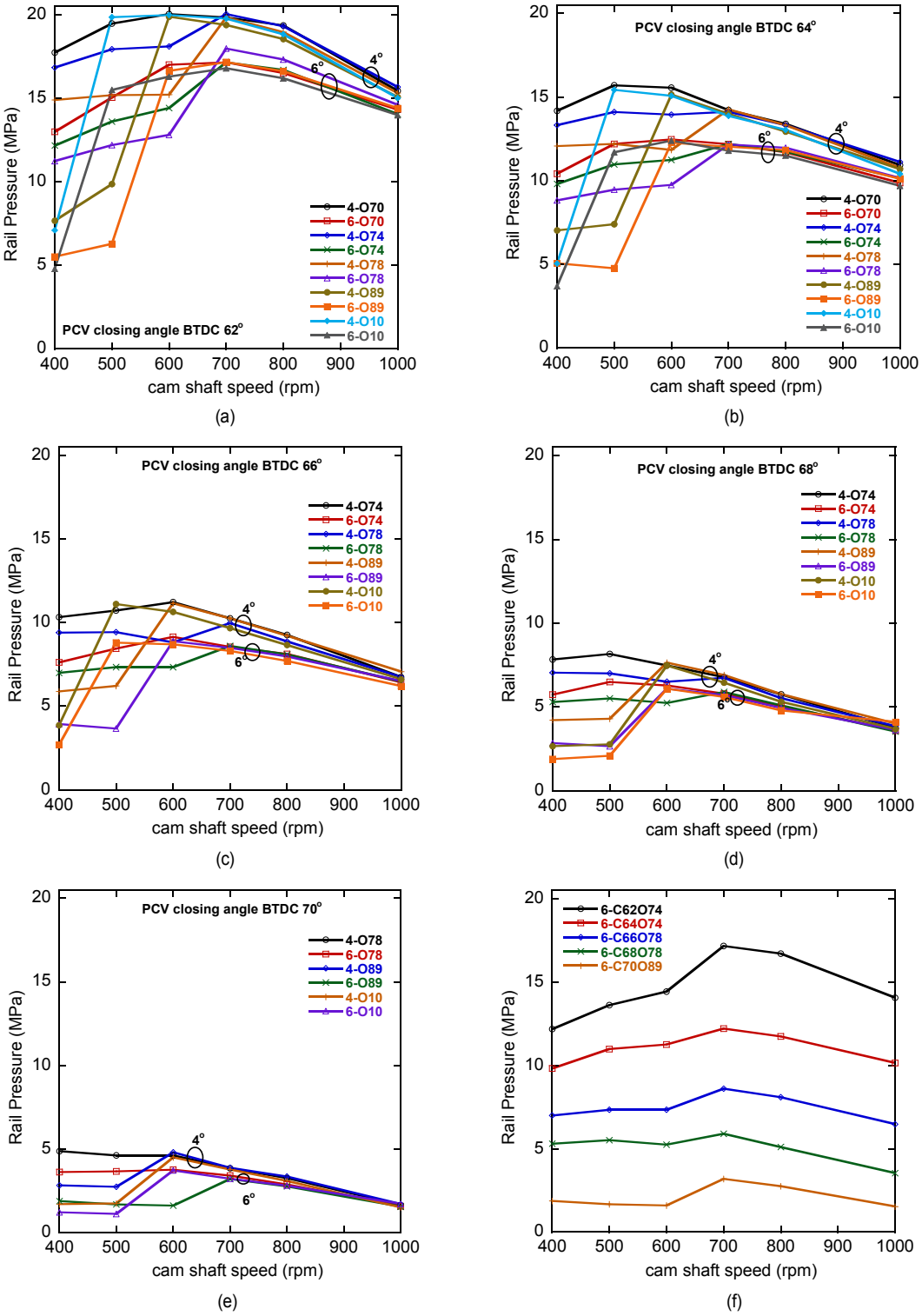

Fig. 4. FRP with camshaft rotation speeds under various conditions of the HPFP PCV valve opening conditions for a fixed PCV closing cam angle: (a) BTDC 62°; (b) BTDC 64°; (c) BTDC 66°; (d) BTDC 68°; (e) BTDC 70°; (f) various closing/opening conditions.

PCV opening angle was small with a fixed HPFP PCV closing angle. In addition, the FRP is clearly divided into two bundles according to fuel injection durations of 4° and 6°. At camshaft speeds of 700-1000 rpm, the FRP with the fuel injection duration angle of 4° was larger than that when the fuel injection duration was 6°. At a camshaft speed of 400-700 rpm, the FRP with a fuel injection duration angle of 4° was also larger than that with a fuel injection duration angle of 6° under the same

PCV opening angle conditions.

As shown in Fig. 4(a), when the PCV opening angle is BTDC 70° and 74°, the FRP change with the camshaft rotational speed was not large. When the PCV opening angle was BTDC 78°, BTDC 89°, and ATDC 10°, the FRP change with the camshaft speed is large in each case, especially in the range of 400-600 rpm. These results stem from the overlap between the fuel injection timing section (BTDC 76°-BTDC 80°) and the pressurized fuel delivery timing section (PCV closing timing section). When the camshaft rotational speed is high, the number of pressurized strokes by the plunger increases, thereby increasing the FRP. With PCV opening timings of BTDC 78°, 89° and ATDC 10°, the FRP did not drop significantly in the high-speed range of 700-1000 rpm.

The results in Figs. 4(b)-(e) are similar to those in Fig. 4(a). However, as the fixed HPFP PCV closing angle increases, the FRP tends to decrease. For stable FRP control under changes in the camshaft rotational speed, it is desirable to control the PCV opening timing before the fuel injection start timing (BTDC 70, 74°).

Figs. 5(a)-(f) show the signal-to-noise ratio (S/N ratio) of FRP under experimental conditions identical to those in Figs. 4(a)-(f). In this experiment, for all experimental conditions, the FRP was measured at 1/5000 second intervals and the sample number of the FRP measurements are 100000. The FRP sample number 100000 are sufficient data which can be regarded as a population. The S/N ratio was calculated by Eq. (1) which divides the average of the FRP by the FRP standard deviation. If the S/N ratio is larger for the same average FRP, it means that the FRP fluctuation is smaller and thus the fluctuation of the fuel injection rate can be expected to be smaller.

$$\frac{S}{N}\ \text{ratio} = \frac{\text{FRP average}}{\text{FRP standard deviation}}\ . \tag{1}$$

The characteristics of the FRP S/N ratio in each experimental condition are related to the FRP and PCV opening/closing timing. Fig. 5(a) shows the results of the FRP S/N ratio according to the cam shaft speed and PCV opening angle changes with a fixed PCV closing angle of BTDC 62°. When the cam shaft speed is in the range of 700-1000 rpm, there is no significant change in the FRP (refer to Fig. 4(a)) according to the change in the PCV opening timing, but the change in the FRP S/N ratio is large. Analyzing only the condition with a fuel injection duration of 4°, when the PCV opening angle is O10, O70, O74, the S/N ratio shows nearly identical values, though there is a large change in the FRP S/N ratio at O78 and O89. In addition, the FRP S/N ratio at O78 and O89 shows smaller values than those at O10, O70, and O74. Therefore, control with O10, O70, and O74 is preferable when generating the same FRP. Analyzing only the conditions with a fuel injection duration of 6°, when the PCV opening angle is O70 or O74, the FRP S/N ratio has nearly the same value. In addition, the FRP S/N ratio at O10, O78, and O89 shows a larger change with the camshaft speed and is smaller than those at O70 and O74. The PCV closing ranges with fuel injection durations of 4° and 6° are BTDC 74°-78° and BTDC 74°-80°, respectively. At PCV opening angles of O74 and O78, the S/N ratio was found to be relatively high because there was no overlap between the fuel injection duration and the PCV closing duration. The PCV opening angle conditions under which the FRP S/N ratio changes with the fuel injection duration are larger are O10 and O89. At a fuel injection duration of 6°, as the fuel injection duration increases, the overlap between the fuel injection duration and the PCV closing duration increases. Thus, the FRP S/N ratio in the O10 and O89 conditions, in which the overlap is greater, decreased significantly compared to the outcomes in the O74 and O78 conditions.

In the camshaft speed range of 400-700 rpm, the change in the FRP ratio with the PCV opening angle and injection duration conditions is larger than those in the range of 700-1000 rpm. In addition, because the cam shaft speed is in the low-speed range, the absolute time corresponding to the same cam angle also increases compared to the high-speed (700-1000 rpm) range. For this reason, in the camshaft speed range of 400-700 rpm, the FRP and FRP S/N ratio changes with the camshaft speed are larger under identical PCV opening/closing angle conditions. The FRP S/N ratio increases with the FRP. Note that the FRP S/N ratio corresponding to the FRP value at 600 rpm shows a smaller value compared to those at other camshaft speeds. That is, the FRP fluctuation at 600 rpm was greater than those at other camshaft speeds. During the experiment, the fluctuation of the FRP at 600 rpm was directly observed through the extreme angle change of a Bourdon tube pressure gauge indicator needle.

Fig. 5(b) shows the results of the FRP S/N ratio with changes in the camshaft speed and PCV opening angle under a fixed PCV closing angle of BTDC 64°. Overall, this condition shows characteristics very similar to those in Fig. 5(a). However, due to the low value of the FRP, the overall FRP S/N ratio showed smaller values compared to those in Fig. 5(a).

Figs. 5(c) and (d) show the results of the FRP S/N ratio with the camshaft speed and PCV opening angles with fixed PCV closing angles of BTDC 66° and BTDC 68°, respectively. Unlike the results in Figs. 5(a) and (b), the FRP was not formed well at the PCV opening angle of O70; accordingly, the experiment was not conducted. Overall, the characteristics of the FRP S/N ratio are similar to those shown in Figs. 5(a) and (b).

Fig. 5(e) shows the results of the FRP S/N ratio with the camshaft speed and PCV opening angle at a fixed PCV closing angle of BTDC 70°. The FRP was again not well formed at the PCV opening angles of O74 and O70. The characteristics of the FRP S/N ratio with the PCV opening angle follow those of the FRP change. The FRP S/N ratio shows nearly identical values in the camshaft speed range of 700-1000 rpm. It can be seen that only under the condition of a PCV opening angle of O78 and injection duration of 4°, the FRP S/N ratio is larger than those under other conditions. This result arises because there is no overlap between the injection duration and the PCV closing duration under the O78 condition, and the fuel injection

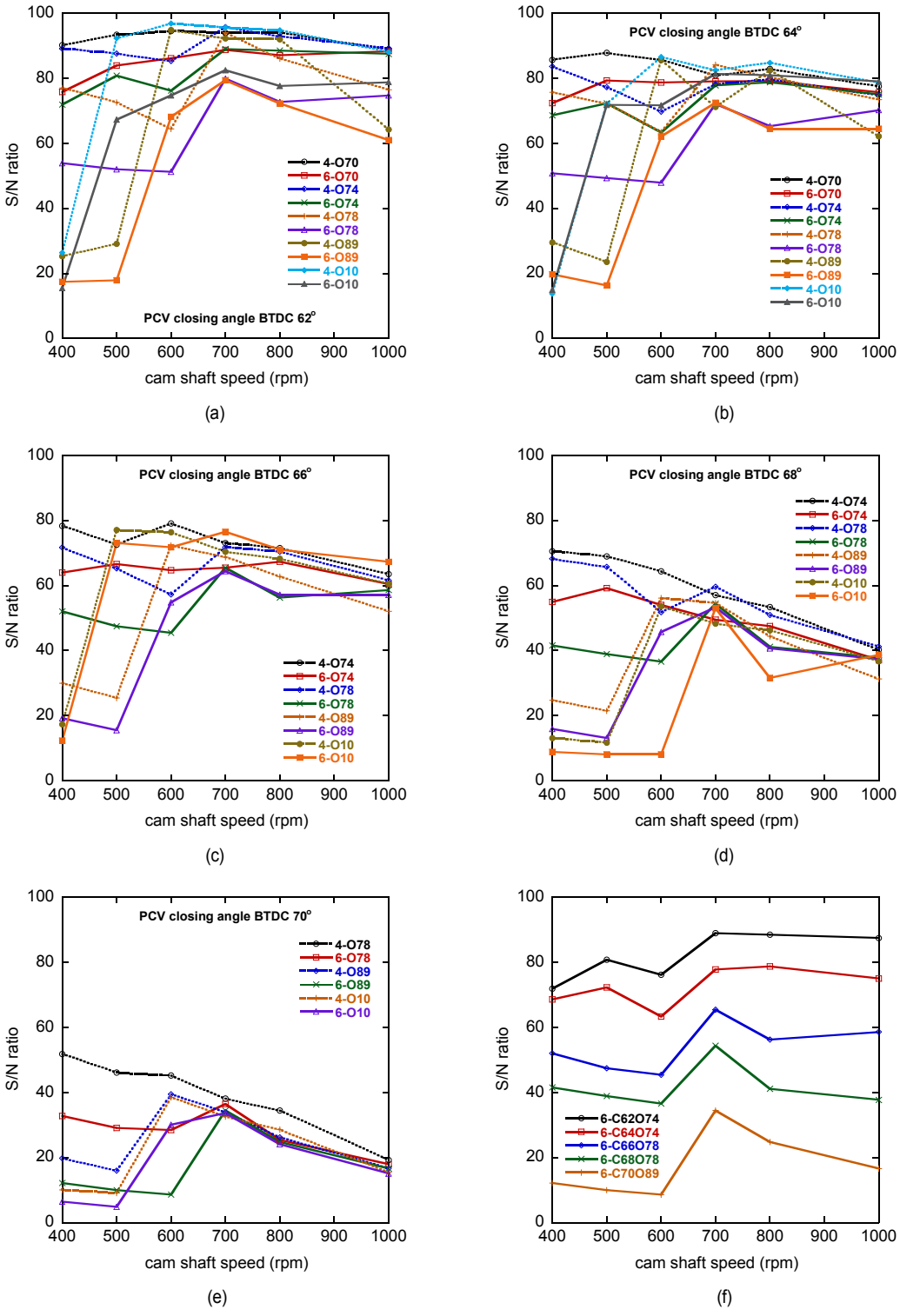

Fig. 5. FRP signal-to-noise ratio with the camshaft rotation speeds under various HPFP PCV valve opening conditions for fixed PCV closing cam angles of: (a) BTDC 62°; (b) BTDC 64°; (c) BTDC 66°; (d) BTDC 68°; (e) BTDC 70°; (f) various closing/opening conditions.

duration is relatively short.

In order to compare the S/N ratios, it is important to calculate the S/N ratios at the experimental conditions where the rail pressure is relatively similar. In addition, the FRP fluctuations were larger at 600 rpm. Fig. 4(f) shows the FRP change according to the camshaft rotation speed change with the various PCV opening/closing conditions. At camshaft rotational speeds of 400, 500, and 600 rpm, the FRP is almost the same, or in-

Table 2. PCV closing and opening angles for the measurement of the fuel injection rate of the GDI injector.

Exp. no.	PCV closing (C) and opening (O) angle (°)
1	C62O10
2	C62O70
3	C62O74
4	C62O78
5	C62O89
6	C64O10
7	C64O70
8	C64O74
9	C64O78
10	C64O89
11	C66O10
12	C66O70
13	C66O74
14	C66O78
15	C66O89
16	C68O10
17	C68O74
18	C68O78
19	C68O89
20	C70O10
21	C70O78
22	C70O89

Table 3. Numbers of injections at each cam shaft speed during six seconds.

Cam shaft speed (rpm)	400	600	800	1000
Injection duration (ms)	1.67	1.11	0.83	0.67
Number of injection during 6 seconds	160	240	320	400

creases slightly as it increases to 500, 600 rpm. Fig. 5(f) shows the S/N ratios corresponding to the same operating conditions shown in Fig. 4(f). Although the rail pressure at 600 rpm is higher than that at 500 and 400 rpm, the S/N ratio at 600 rpm is relatively smaller than that at 400 and 500 rpm. The smaller S/N ratio means that the FRP variation is larger.

The experimental conditions used in this study are set by combining Tables 2 and 3. For example, with the experiment no. 1 in Table 1 and camshaft speed of 400 rpm in Table 3, the experimental condition is fixed as PCV closing/opening timing of 62 BTDC°/10 ATDC° and fuel injection duration of 1.67 ms. Under these experimental condition, the GDI injector will inject 160 times during six seconds. The collected fuel mass during six seconds measured with a scale is divided by 160, which results in the injected fuel mass of single injection with the GDI injector. The six seconds measurement was repeated 20 times consecutively to statistically analyze the variation in the injected

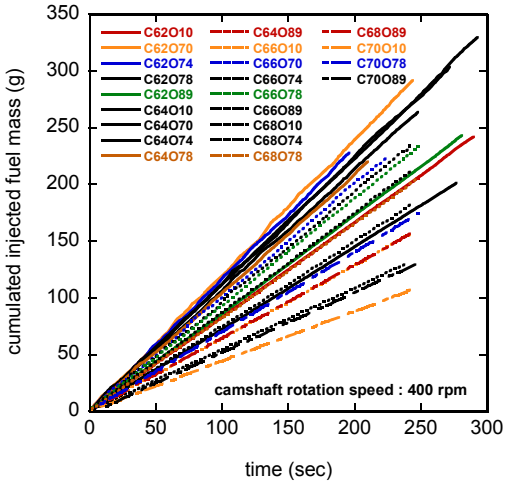

Fig. 6. Cumulated injected fuel mass (CIFM) from a GDI injector at one-second intervals for various experimental conditions (camshaft speed: 400 rpm).

fuel mass. By combining the conditions of Tables 2 and 3, the injector injection rate was repeatedly measured in the manner described above. Total number of experimental conditions performed in this study are 88. The fuel injection rate measurements with the developed experimental system can be expanded for all engine operating conditions. The optimum control condition which show a small variation in the injector injection rate can be determined from the collected data under all the engine operating conditions.

Fig. 6 shows the cumulated injected fuel mass (CIFM) from a GDI injector at one-second intervals for various combinations of PCV closing and opening angles at a camshaft speed of 400 rpm. Under all PCV closing/opening angle combinations shown in Table 2, the CIFM increases linearly with time. In each condition, the slope of the CIFM curve is the injection rate (g/s) of the GDI injector. The curve slope change under each experimental condition is relatively uniform. This means that the FRP can be controlled evenly with the PCV closing/opening angle conditions. The fuel injection duration in ms corresponding to the injection duration 4° at the camshaft speed of 400 rpm is 1.67 ms. Figs. 7-9 show the CIFMs at one-second intervals with various combinations of the PCV closing/opening angles at camshaft speeds of 600, 800, and 1000 rpm, respectively. The CIFM curves in Figs. 7-9 all show linear characteristics similar to those shown in Fig. 6. As the camshaft speed increases, the slope of the CIFM curves does not increase evenly, and they eventually merge into five groups.

Fig. 10 shows the average injected fuel mass during six seconds for the PCV closing/opening conditions summarized in Table 2. The numbers of injections at each cam shaft speed during six seconds are summarized in Table 3. The injected fuel mass per stroke can be obtained by dividing the injected fuel mass during six seconds by the number of injections during six seconds. Fig. 11 shows the injected fuel mass per stroke for all of the experimental conditions summarized in

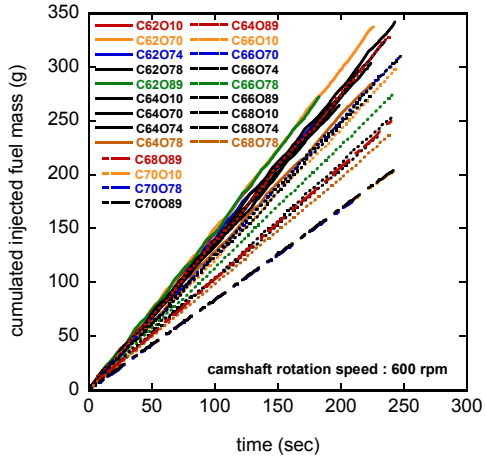

Fig. 7. Cumulated injected fuel mass (CIFM) from a GDI injector at one-second intervals for various experimental conditions (camshaft speed: 600 rpm).

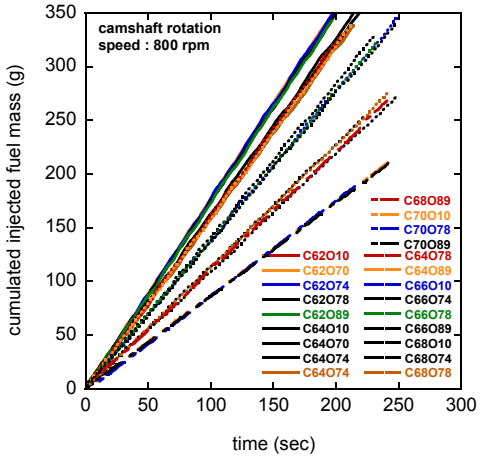

Fig. 8. Cumulated injected fuel mass (CIFM) from a GDI injector at one-second intervals for various experimental conditions (camshaft speed: 800 rpm).

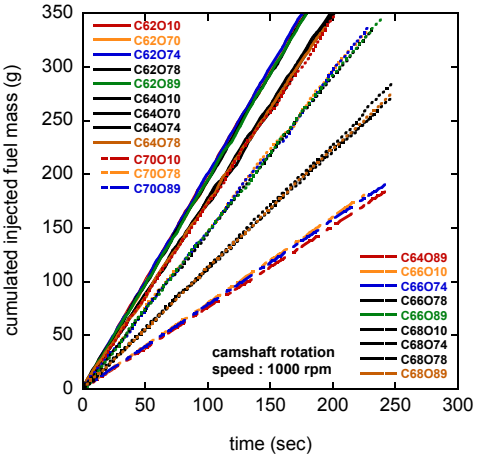

Fig. 9. Cumulated injected fuel mass (CIFM) from a GDI injector at one-second intervals for various experimental conditions (camshaft speed: 1000 rpm).

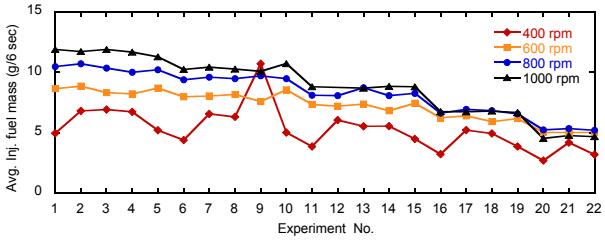

Fig. 10. Average injected fuel mass during six seconds for various PCV closing/opening conditions.

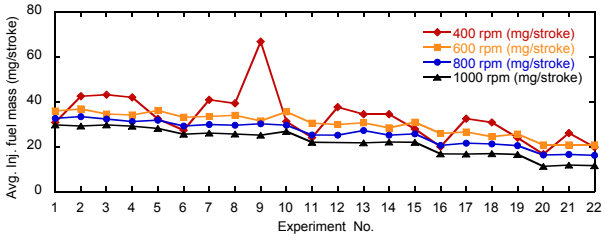

Fig. 11. Average injected fuel mass per stroke for various PCV closing/opening conditions.

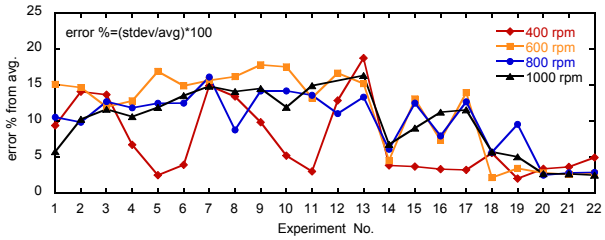

Fig. 12. Error % of the standard deviation from the average value for the injected fuel mass during six seconds.

Table 2.

Fig. 12 shows the error % of the standard deviation from the average value for the injected fuel mass during six seconds. The measurements are repeated 20 times in each of the PCV closing/opening conditions listed in Table 2. The error % shows a distribution of 3-15 %. In the PCV closing angle condition C70, that is, in the case where the closing angle is later, the deviation value is 3 %. These results are related to the lower FRP. With regard to the relationship between the S/N ratio and FRP variation, it was shown that the smaller S/N ratio, the larger FRP variation. The injection rate error % shown in Fig. 12 was generally larger at 600 rpm. Previously, the S/N ratio at 600 rpm appeared to be smaller for a similar FRP. The larger error % of the fuel injection rate is, the smaller S/N ratio is. Thus, if the opening/closing timing of the pressure control valve showing a larger value of the S/N ratio is selected and controlled, the variation of the fuel injection rate can be reduced.

Fig. 13 shows the relationship between the FRP and injection rate calculated from the slopes of the CIFM curves shown in Figs. 6-9. Each curve was fitted at 400 rpm, 600 rpm, 800 rpm, and 1000 rpm. The relationship between the FRP and injection rate can be expressed as a second-order polynomial, and the correlation coefficient for each curve is 0.99 or higher. Table 4

Table 4. Curve fitting equations between the FRP and injection rate at camshaft speeds of 400, 600, 800 and 1000 rpm.

Cam shaft speed	Curve fitting results	R
400 (rpm)	inj rate = -0.002108(FRP)^2+0.085227(FRP)+0.32607	0.9984
600 (rpm)	inj rate = -0.0022893(FRP)^2+0.096129(FRP)+0.44911	0.9967
800 (rpm)	inj rate = -0.0032155(FRP)^2+0.12683(FRP)+0.50386	0.9974
1000 (rpm)	inj rate = -0.004583(FRP)^2+0.16216(FRP)+0.55474	0.9979

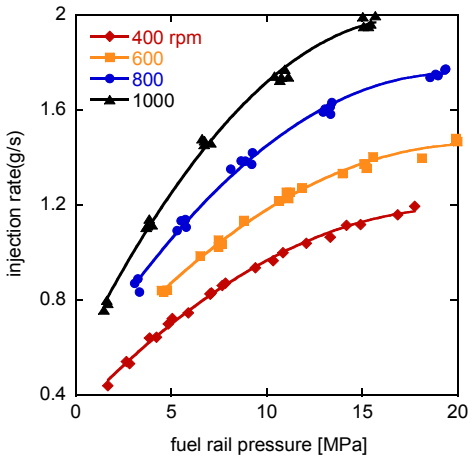

Fig. 13. Curve fitting results between the FRP and injection rate at camshaft speeds of 400, 600, 800 and 1000 rpm.

summarizes the curve fitting equation between the FRP and injection rate at each camshaft speed. Using the GDI fuel injection system developed in this study, the relationship between the injection rate and FRP can be successfully obtained.

4. Conclusions

A system that can accumulate and measure the fuel injected mass from a GDI injector was developed. The fuel injection rate and FRP pulsation were measured under various experimental conditions with various camshaft speeds of the GDI experimental rig, HPFP PCV opening/closing timings, and fuel injection durations and the following results were obtained.

1) The FRP S/N ratio showed a larger value as the FRP increased. Under the same FRP values, the earlier the HPFP PCV closing angle, the shorter the fuel injection duration and the faster the cam shaft speed make the higher the FRP S/N ratio. Moreover, the FRP S/N ratio shows a higher value when avoiding the overlap between the fuel injection duration and the PCV closing duration.

2) The smaller S/N ratio shows the larger FRP variation under the same FRP condition. Also, it was identified that the S/N ratio is related to the variation of the fuel injection rate.

3) The FRP S/N ratio was particularly low at a specific camshaft speed and under a PCV closing/opening condition, and it is desirable to avoid this situation when designing a GDI fuel injection system control scheme.

4) Under the PCV closing/opening conditions, the injection rate could be obtained from the slope of the CIFM curve over time. The curve fitting of the relationship between the injection rate and the FRP obtained under each experimental condition could be expressed as a second-order polynomial, and the correlation coefficient for each curve was 0.99 or higher. It was shown that a map of the FRP and injector injection rate can be obtained through such an experimental process.

Acknowledgments

This study was supported by the Research Program funded by the Seoul National University of Science and Technology.

References

[1] A. A. Reddy and J. M. Mallikarjuna, Parametric study on a gasoline direct injection engine - A CFD analysis, *SAE Paper 2017-26-0039* (2017).

[2] F. Q. Zhao and M. C. Lai, A review of mixture preparation and combustion control strategies for spark-ignited direct-injection gasoline engines, *SAE Paper 970627* (1997).

[3] R. Golzari, Y. Li and H. Zhao, Impact of port fuel injection and in-cylinder fuel injection strategies on gasoline engine emissions and fuel economy, *SAE Paper 2016-01-2174* (2016).

[4] J. G. Spakowski, J. Kazour, B. C. Kaswer, M. Harstad and T. D. Spegar, GDI high efficiency fuel pump for fast engine starts and reduced cam loads, *SAE Paper No. 2019-01-1196* (2019).

[5] Robert Bosch GmbH, *Diesel Engine Management*, 4th Ed., Bentley Publishers (2005).

[6] F. Q. Zhao, M. C. Lai and D. L. Harrington, Automotive spark-ignited direct-injection gasoline engines, *Progress in Energy and Combustion Science*, 25 (2016) 437-562.

[7] E. A. Rivera, N. Mastro, J. Zizelman, J. Kirwan and R. Ooyama, Development of injector for the direct injection homogeneous market using design for six sigma, *SAE Paper 2010-01-0594* (2016).

[8] M. Cavanagh, R. Pellini and S. J. Pinson, Advances in gasoline direct injection fuel pump technologies, *SAE Paper 2018-01-0367* (2018).

[9] H. Zhao, *Advanced Direct Injection Combustion Engine Technologies and Development*, Cambridge: Woodhead Publishing Limited (2010).

[10] C. Wang, H. Xu, J. M. Herreros, J. Wang and R. Cracknell, Impact of fuel and injection system on particle emissions from a GDI engine, *Applied Energy*, 132 (2014) 178-91.

[11] R. Payri, G. Bracho, J. Gimeno and A. Bautista, Rate of injection modelling for gasoline direct injectors, *Energy Conversion and Management*, 166 (15) (2018) 424-432.

[12] H. Husted, T. D. Spegar and J. Spakowski, The effects of GDI fuel pressure on fuel economy, *SAE Paper 2014-01-1438* (2014).

[13] Q. Liu, H. Chen, Y. Hu, P. Sun and J. Li, Modeling and control of the fuel injection system for rail pressure regulation in GDI engine, *IEEE/ASME Transactions on Mechatronics*, 19 (5)

(2014) 1501-1513.
[14] T. D. Spegar, S. I. Chang, S. Das, E. Norkin and R. Lucas, An analytical and experimental study of a high pressure single piston pump for gasoline direct injection (GDI) engine applications, *SAE Paper 2009-01-1504* (2009).
[15] T. D. Spegar, Minimizing gasoline direct injection (GDI) fuel system pressure pulsations by robust fuel rail design, *SAE Paper 2011-01-1225* (2011).
[16] K. Hiraku, K. Tokuo and H. Yamada, Development of high pressure fuel pump by using hydraulic simulator, *SAE Paper 2005-01-0099* (2005).
[17] J. M. Lee and C. H. Lee, A development of fuel rail pressure control system for evaluating GDI injector performance, *KSAE Spring Conference*, 18KSAE-B003 (2018).
[18] B. J. Lee and C. H. Lee, Fuel rail pressure control characteristics of a GDI high pressure fuel pump using a newly developed experimental system controlled with a microcontroller, *International Journal of Automotive Technology*, 22 (2) 489-497 (2021).
[19] *Surface Vehicle Recommended Practice: Low Pressure Gasoline Fuel Injector*, J1832, SAE International (2016).
[20] *Surface Vehicle Recommended Practice: Direct Injection Gasoline Fuel Injector Characterization*, J2713, SAE International (2018).

Lee, Byoung-Jin received his B.S. (2019) in Department of Automotive Engineering at Seoul National University of Science and Technology. His research interests are flow measurements and control of fuel injection system in automotive. He has worked in Samsung Electronics Co. Ltd since 2020.

Lee, Choong-Hoon received his B.S. (1985), M.S. (1987), and Ph.D. degrees (1996) in Mechanical Engineering from Seoul National University. He worked as a diesel engine development engineer for Daewoo Heavy Industry for six years. He was a visiting research fellow at the Engine Research Center at the University of Wisconsin-Madison in 1997. He has worked in the Department of Automotive Engineering at Seoul National University of Technology as a Professor since 2000. His research interests are the measurement and control of sprays and flows.